archives
of thermodynamics
Vol. **32**(2011), No. 2, 55–68
DOI: 10.2478/v10173-011-0009-1

A definition of near-critical region based on heat capacity variation in transcritical heat exchangers

MARIAN TRELA*
ROMAN KWIDZIŃSKI
DARIUSZ BUTRYMOWICZ

The Szewalski Institute of Fluid Flow Machinery of the Polish Academy of Sciences, Fiszera 14, 20-231 Gdańsk, Poland

Abstract In the paper, a method for determination of the near-critical region boundary is proposed. The boundary is evaluated with respect to variations of specific heat capacity along isobars. It is assumed that the value of specific heat capacity inside the near-critical region exceeds by more than 50% the practically constant value typical for fluids under normal conditions. It appears that large variations of heat capacity are also present for high-pressure subcritical states sufficiently close to the critical point. Therefore, such defined near-critical region is located not only in supercritical fluid domain but also extends into subcritical fluid. As an example, the boundaries of the near-critical region were evaluated for water, carbon dioxide and R143a.

Keywords: Critical thermodynamic state; Near-critical region; Heat transfer; Specific heat capacity

Nomenclature

c_p	–	specific heat capacity at constant pressure, J/kg K
E_q	–	relative work of thermal expansion
h	–	specific enthalpy, J/kg

*Corresponding author. E-mail address: mtr@imp.gda.pl

$\dot{m}$ – mass flow rate, kg/s
p – pressure, Pa
T – temperature, K
s – specific entropy, J/kg K
v – specific volume, m^3/kg

Greek symbols

β – coefficient of thermal expansion, 1/K
λ – thermal conductivity, W/m K
ρ – density, kg/m^3

Subscripts

b – at near-critical region boundary
c – at critical point
o – organic fluid
pc – pseudocritcal
w – water

1 Introduction

In an increasing tendency to improve the efficiency of energy conversion, heat transfer to fluids in near-critical thermodynamic state is of great importance. Recently, near-critical or supercritical Rankine cycles have been studied for wide selection of fluids such as water, carbon dioxide and organic refrigerants. As an example, studies of supercritical Rankine cycle for coal-burned turbine unit [1] can be recalled. Also, supercritical Organic Rankine Cycle (S-ORC) can be mentioned [2], which could be applied to produce electricity from renewable low-temperature heat sources. Recently, special attention has also been paid to carbon dioxide refrigeration cycles which may be near-critical or supercritical (for the conventional systems and heat pumps) or subcritical (for the cascade systems) [3].

Due to large variations of thermodynamic and transport properties of the fluids in the vicinity of critical point, classical methods of heat exchanger design fail to predict correctly the temperature changes along the exchanger. As a result of large increase of the heat capacity, the temperature difference between the fluids may become unacceptably small at some point inside the exchanger if the temperature difference assumed at the exchanger inlet is too small. Anomalies of heat capacity and other fluid properties are distinctive feature of the so-called near-critical region. These anomalies together with buoyancy forces cause instabilities and other heat transfer peculiarities in pipe flow inside the exchanger [4,5]. Unfortunately, the extent and limits of

the near-critical region are not clearly distinguished and variously referred to in the literature.

In the paper we propose a definition of the near-critical region that is based on variations of specific heat capacity along isobars. Use of variables reduced with respect to the critical parameters ensures that, according to the principle of corresponding states, the proposed method yields similar results for a variety of fluids. As an example, the near-critical region boundaries are determined for water, carbon dioxide and R143a.

2 Fluid properties and heat transfer near the critical point

Irregularities in heat transfer are observed in heat exchangers working under supercritical pressures [4]. They arise from large variations of fluid physical properties in near-critical region. Some examples of these variations are shown in Figs. 1 and 2. Specific heat capacity at constant pressure c_p, thermal conductivity λ and coefficient of thermal expansion β rise to very large or infinite values at critical point, while density value sharply drops. Such anomalies appear not only at critical isobar p_c (Fig. 1) but are also observed for a range of pressures close to the critical one. As an example, in Fig. 2 are depicted c_p isolines near the critical point showing that this property reaches high values for a range of pressures and temperatures below and above the critical state. In supercritical region, the maximum value of c_p for a given pressure determines the pseudocritical temperature T_{pc} (also called the transposed critical temperature).

Bearing in mind a definition of c_p,

$$c_p \equiv \left(\frac{\partial h}{\partial T}\right)_p , \tag{1}$$

it is easy to see in the T-h diagram that the more the isobar departs from a straight line, the more c_p value varies along it. Also, when the slope of the isobar diminishes, the c_p value rises, reaching infinity at critical point.

Variations of c_p value are one of the reasons for irregularities in temperature profile along the supercritical heat exchanger. In this case, the average temperature difference between fluids differs substantially from logarithmic mean. It will be illustrated using data for supercritical ORC module analyzed in [2]. This S-ORC module is meant to utilize the heat of water cooling a biogas engine to generate additional electric power. One of the

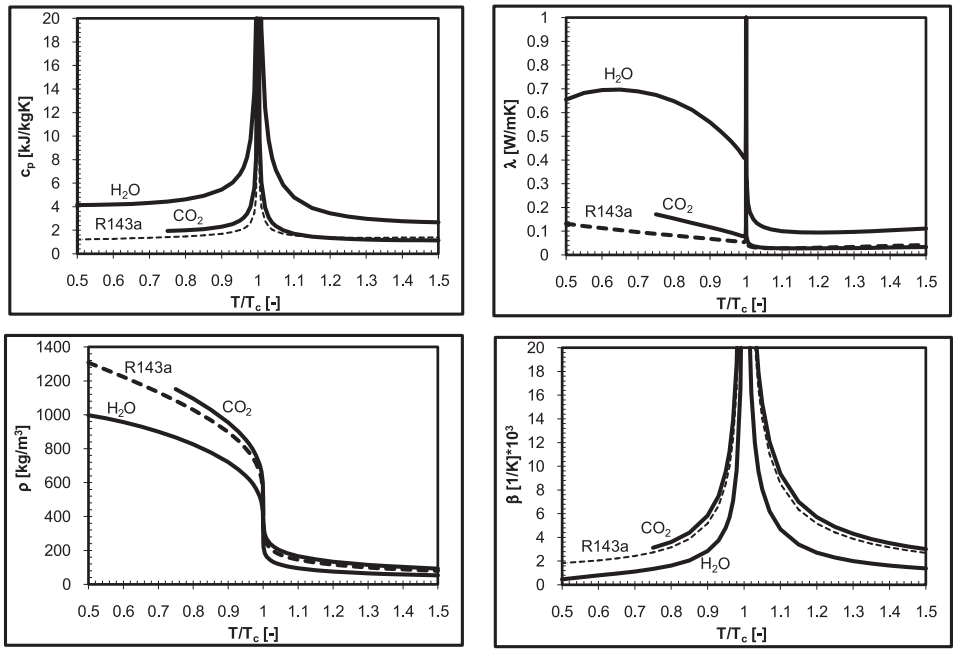

Figure 1. Distributions of specific heat capacity at constant pressure c_p, thermal conductivity λ, density ρ and coefficient of thermal expansion β along critical isobar as a function of reduced temperature T/T_c. Properties of three fluids are shown: water (H_2O, $p_c = 22.06$ MPa, $T_c = 647.1$ K), carbon dioxide (CO_2, $p_c = 7.38$ MPa, $T_c = 304.1$ K) and R143a ($p_c = 3.76$ MPa, $T_c = 345.9$ K) [7].

organic working fluids proposed was R143a (1,1,1-trifluoroethane), which would undergo isobaric heating in the exchanger. It was assumed that the heating water enters the exchanger at temperature 90 °C and flow rate 34 m^3/h. The water temperature at the exchanger outlet should be 63 °C. The temperature difference between water and R143a at the hot end of the exchanger was assumed to be 5 °C. Its inlet temperature resulted from an assumption that the working fluid would be compressed isentropically in a circulation pump from saturated state at 30 °C to the exchanger working pressure, which should have a value selected from a range 3.8–4.6 MPa. The flow rate of R143a was adjusted to obtain required temperature drop of water in the exchanger. T-s diagram for the analyzed S-ORC cycle is shown in Fig. 3, which also introduces the numbering of thermodynamic states at its characteristic points[1]. Thus, for the heat transfer in the exchanger, simple

[1]It can be noted that for high working pressures of R143a, the expansion falls deep

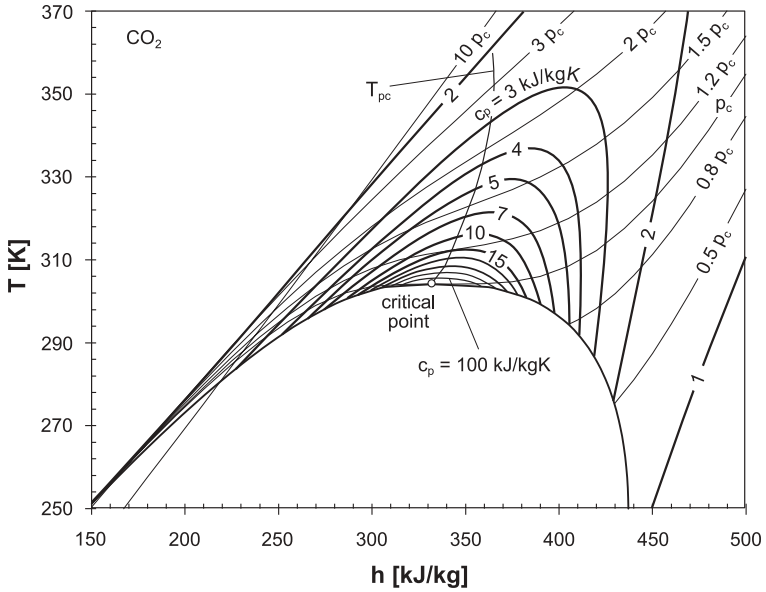

Figure 2. T-h diagram for CO_2 with isobars (thin lines) and c_p isolines (bold lines) plotted in the vicinity of the critical point. The pseudocritical temperature T_{pc} line is also shown.

global heat balance can be written in the form

$$\dot{m}_w \left(h_{w1} - h_{w2}\right) = \dot{m}_o \left(h_{o1} - h_{o4}\right). \tag{2}$$

Similar balances are valid for heat transfer between the water and R143a in any control volume confined by two control cross-sections set along the analyzed supercritical exchanger. In particular, for constant flow rates, this control cross-sections can divide the exchanger into a number of segments in which equal portions of the total enthalpy change are transferred for each fluid. The energy balance for a segment between control cross-sections i an $i+1$ can be written as

$$\dot{m}_w \left(h_w^i - h_w^{i+1}\right) = \dot{m}_o \left(h_o^{i+1} - h_o^i\right) , \tag{3}$$

where

$$h_w^i - h_w^{i+1} = \frac{h_{w1} - h_{w2}}{n} \quad \text{and} \quad h_o^{i+1} - h_o^i = \frac{h_{o1} - h_{o4}}{n}, \quad i = 0, 1, \ldots, n \, . \tag{4}$$

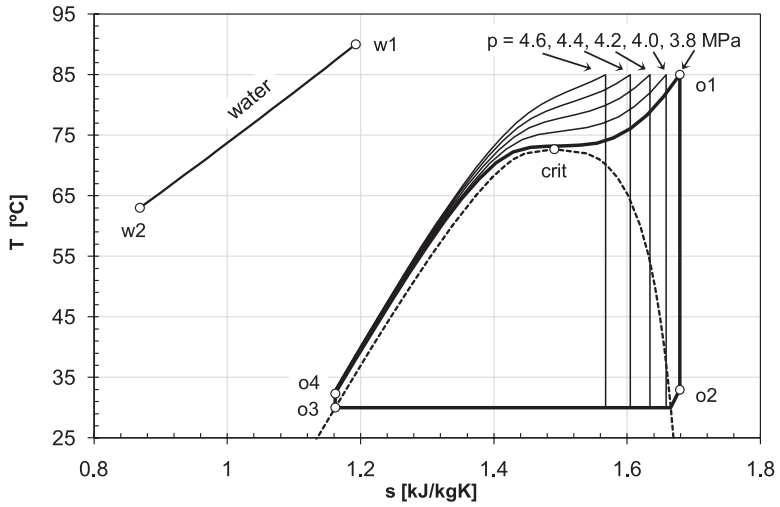

Figure 3. T-s diagram for supercritical ORC cycle analyzed in [2] with water and R143a as a working fluid.

Starting from one end of the exchanger and using (3) successively for all segments, the enthalpies h_w^i and h_o^i can be calculated. Then the temperatures of working fluids in the control cross-sections along the exchanger can be determined. The results of such calculations for $n = 20$ segments are depicted in Fig. 4. It is clearly seen, that temperature difference between water and R143a changes in a irregular way, especially in a high-temperature part of the exchanger. In this part of the exchanger, the heat capacity c_p values are much higher than in the regions where fluid properties are distant from the critical point, Fig. 4c. Also, the temperature difference at some points inside the exchanger is lower than at its high-temperature end, particularly for R143a pressures close to critical value.

It should be noted that the profiles shown in Fig. 4b are independent of the exchanger geometry. Each segment considered here will generally comprise different lengths of the exchanger, depending on local heat transfer conditions. Determination of temperature profiles as a function of the exchanger length is of course possible, provided the appropriate correlations for the heat transfer coefficient will be used.

into a wet steam region. In such case a screw expander should be used instead of a turbine in the S-ORC module.

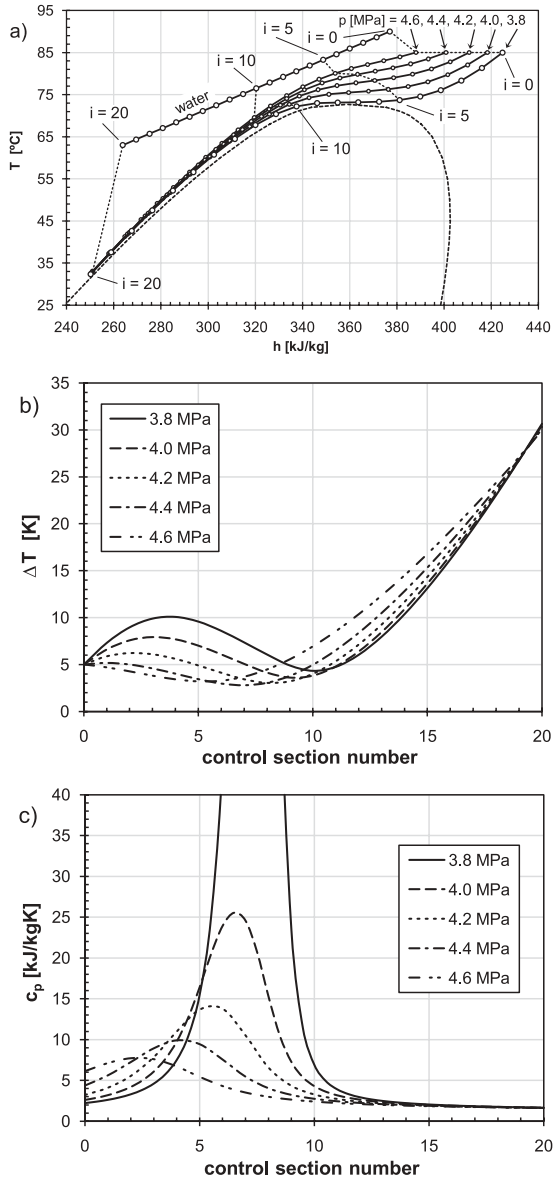

Figure 4. Calculations of temperature profiles along the supercritical heat exchanger: a) T-h diagram showing isobars for the working fluids – water at atmospheric pressure and R143a under selected supercritical pressures; dots indicate the partition of the exchanger into $n = 20$ control segments of equal enthalpy increments; broken lines connect corresponding cross sections for $i = 0$, $i = 5$, $i = 10$ and $i = 20$ in both fluids; b) temperature differences between working fluids in the exchanger control segments for the considered pressure values of R143a; c) variation of R143a heat capacity c_p along the exchanger, which reaches a maximum value of 157 kJ/kgK for $p = 3.8$ MPa.

3 Definition of near-critical region

As has been shown above, fluid properties in the vicinity of critical point change substantially. However, the transitions are not sharp so the demarcation of near-critical region boundary is difficult. In some papers this region is characterized by the pressure and temperature conditions. For example, in [5] the near-critical region for hydrogen is described by the pressure range $0.8 < p/p_c < 3$ and two conditions for temperature: the lowest temperature is set at saturation line corresponding to $p/p_c = 0.8$ and the upper temperature boundary is located at an indefinite line above the pseudocritical temperature connecting the isobars $0.8p_c$ and $3p_c$. In other works (e.g. Kurganov [6]), a non-dimensional quantity

$$E_q = p\left(\frac{\partial v}{\partial h}\right)_p = p\frac{\beta}{\rho c_p}\,, \tag{5}$$

called the relative work of thermal expansion, is used instead of temperature to distinguish the near-critical fluid from subcritical liquid and supercritical gas regions. The value of the relative work of thermal expansion E_q is almost independent of pressure, especially for temperature (or enthalpy) far from critical value, see Fig. 5.

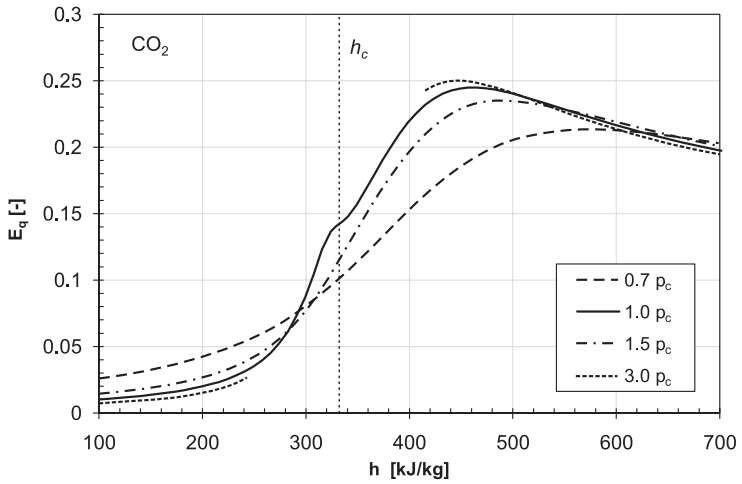

Figure 5. Profiles of relative work of thermal expansion E_q for carbon dioxide (CO_2) under selected pressures. Vertical line denotes the value of critical enthalpy h_c.

Along the isobar, E_q is almost constant for a low-temperature liquid but starts to rise as the temperature approaches the critical or pseudocritical value. Beginning of the rise, set here at $E_q = 0.04$, is considered by Kurganov as the lower boundary of near-critical region. Beyond the (pseudo)critical temperature, the E_q attains maximum that is considered the higher boundary of the region. Further up, E_q value diminishes slowly with temperature.

In this paper, more precise definition of the near-critical region boundary (NRB) is proposed. It is based on variations of specific heat capacity c_p along isobars. The NRB is determined in relation to the pseudocritical temperature T_{pc} and the critical temperature T_c. Use of the critical temperature ensures that the proposed method yields similar results for a variety of fluids. Because large variations of c_p are also present in subcritical domain, the saturation temperature T_{sat} is used instead of T_{pc} to determine NRB there.

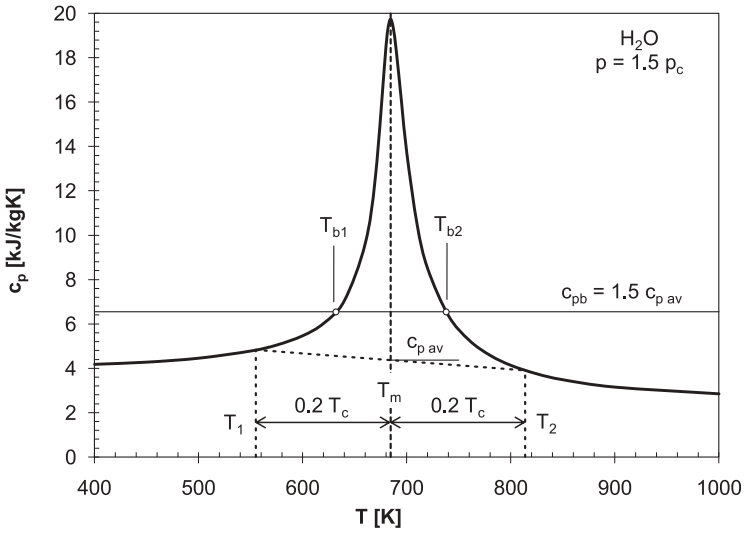

Figure 6. A method of determination of temperatures T_{b1} and T_{b2} that mark near-critical segment of heat capacity c_p variation along a selected isobar.

Determination of NRB by the proposed method will be explained with the help of Fig. 6. First, for each isobar passing in the vicinity of critical

point, the temperature T_m at which the heat capacity c_p reaches maximum should be found. The T_m equals to pseudocritical temperature T_{pc} if $p > p_c$, the critical temperature T_c when $p = p_c$ or the saturation temperature T_{sat} for $p < p_c$. Then, two values of c_p are found at temperatures $T_1 = T_m - fT_c$ and $T_2 = T_m + fT_c$, where f is a fraction assumed to be $f = 0.2$. Next, limiting heat capacity c_{pb} which determines NRB points at the selected isobar P is found. It is proposed that the c_{pb} value is equal to 150% of the arithmetic average of heat capacities at the temperatures T_1 and T_2, i.e.

$$c_{pb}\left(p, T_{b1}\right) = c_{pb}\left(p, T_{b2}\right) = 1.5\,\frac{c_p\left(p, T_1\right) + c_p\left(p, T_2\right)}{2} = 1.5 c_{p\,av}\,. \qquad (6)$$

When the c_{pb} is known, the corresponding lower and upper temperatures at the boundary, designated T_{b1} and T_{b2} in Fig. 6, can be found. After repeating this procedure for a number of isobars the complete NRB line can be drawn. It starts at the saturation lines and crosses the isobars up to $\approx$ 2.5–3 p/p_c. For higher pressures the maximum of c_p diminishes so much that $c_{pmax} < c_{pb}$.

4 Near-critical region for selected fluids

Example calculations of NRB were performed for water (H_2O), carbon dioxide (CO_2) and R143a (1,1,1-trifluoroethane). Thermodynamic properties of these fluids were calculated using REFPROP 8 database [7]. The results are depicted in Figs. 7a–7c. Besides the NRB determined by the present method, the lines of $E_q = 0.04$ and $E_q = \max$ are also shown. They mark the near-critical region according to Kurganov criterion [6].

The NRB determined by the method proposed here has a similar shape for the three fluids considered, see Fig. 8. The boundary designates a region which also extends into subcritical fluid domain. The extent of the near-critical region is largest for water, covering pressures in the range $0.25 < p/p_c < 3.04$ and temperatures $0.84 < T/T_c < 1.21$. For carbon dioxide these intervals are $0.35 < p/p_c < 2.46$ and $0.85 < T/T_c < 1.17$. For the last fluid considered, the R143a, near-critical region is smallest and is bounded by $0.55 < p/p_c < 2.18$ and $0.92 < T/T_c < 1.14$.

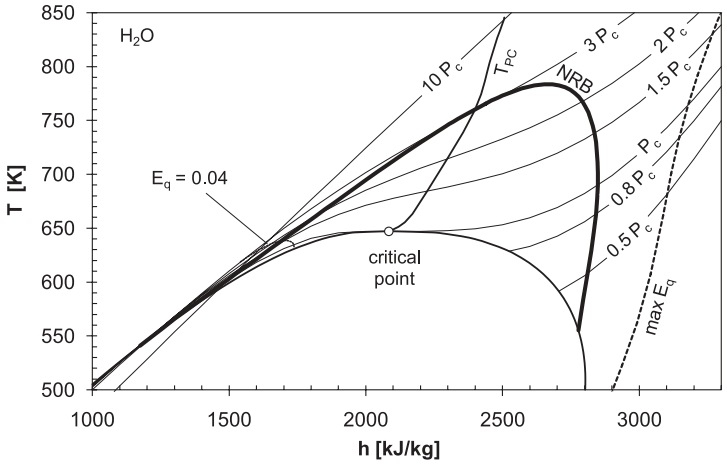

Figure 7a. T-h diagram for water showing the near-critical region boundary (NRB) determined by the present method. Also shown are isobars, pseudocritical temperature line (T_{pc}) and the lines of relative work of thermal expansion (E_q) marking the near-critical region according to Kurganov [6].

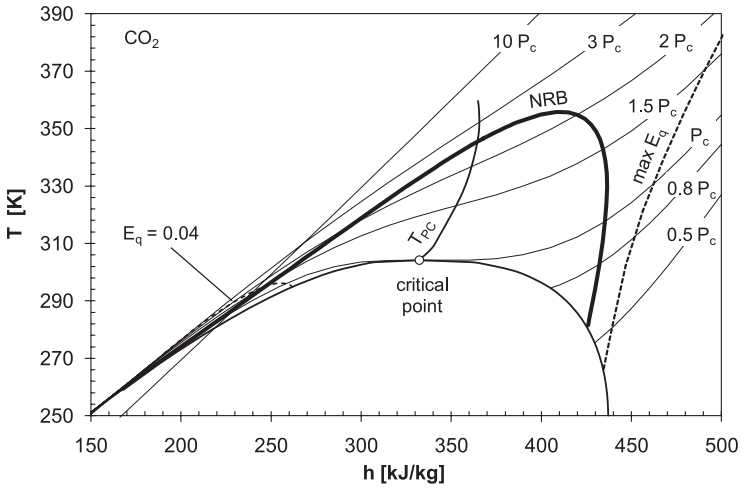

Figure 7b. T-h diagram for carbon dioxide showing the near-critical region boundary (NRB) determined by the present method. Other lines as in Fig. 7a.

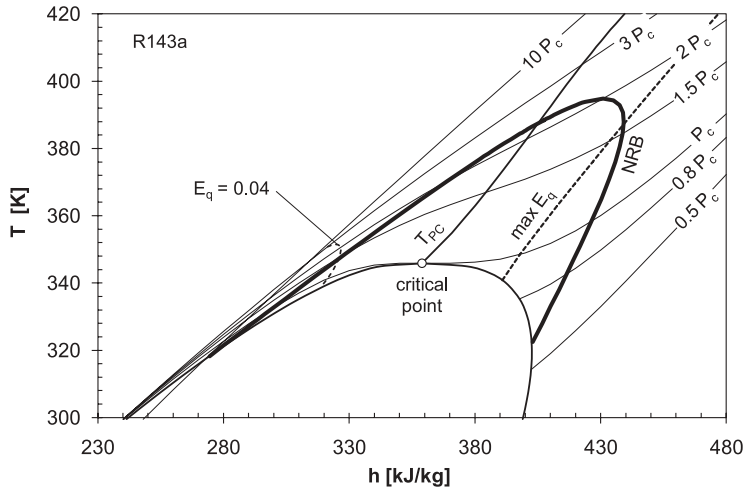

Figure 7c. T-h diagram for R143a showing the near-critical region boundary (NRB) determined by the present method. Other lines as in Fig. 7a.

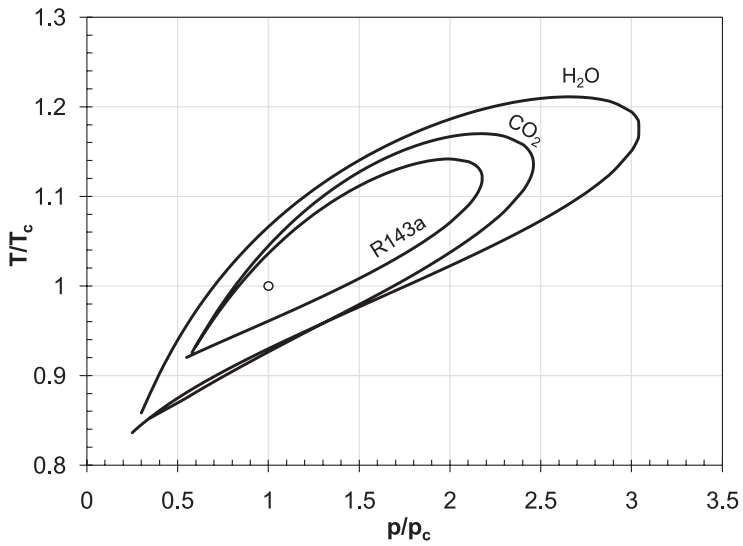

Figure 8. The boundaries of near-critical regions for water (H_2O), carbon dioxide (CO_2) and R143a compared in non-dimensional p-T coordinates.

5 Conclusions

A simple and more rational definition of the near-critical region is proposed in the paper. The boundary of this region (NRB) is evaluated with respect to variations of specific heat capacity along isobars that pass in the vicinity of critical point. It is assumed that the values of constant-pressure heat capacity c_p inside the near-critical region are greater than 150% of the practically constant value which is typical for fluids under normal conditions. It appears that the near-critical region is located not only in supercritical fluid domain but also extends into subcritical fluid. This is a result of large heat capacity variations that are observed for high-pressure subcritical states which are sufficiently close to the critical point.

The knowledge of NRB is particularly important during design of heat exchangers working with near-critical fluids. In such case, special attention should be paid to calculations of temperature difference between the working fluids. Reliable results can be obtained only if heat balances are written for small segments of the exchanger where the heat capacity value can be considered to remain constant. Moreover it should be noticed that in many experiments on heat transfer under near-critical conditions, degradation of local heat transfer coefficient and flow pulsations were reported, especially in flows in vertical pipes.

Acknowledgement This paper was prepared as a part of the Szewalski Institute of Fluid-Flow Machinery of the Polish Academy of Sciences statutory activities within the framework of O2/T3 theme.

Received 7 July 2011

References

[1] Chmielniak T., Ziębik A. (Eds.): *Supercritical Coal Based Steam Cycles*. Publishing House of Silesian University of Technology, Gliwice 2010 (in Polish).

[2] Borsukiewicz-Gozdur A., Nowak W.: *Increasing of electricity generation capacity of biogas power generator by application of sub- and supercritical modules of Organic Rankine Cycle*. Archives of Thermodynamics **30**(2009), 4, 3–17.

[3] Angielczyk W., Butrymowicz D., Bartosiewicz Y., Dudar A.: *Analysis of transcritical CO_2 refrigeration cycle with two-phase ejector*. In: Proc. 5th International Conference on Transport Phenomena In Multiphase Systems (HEAT 2008), Vol. 2, June 30–July 3, 2008, Białystok, Poland, 403–410.

[4] Polyakov A.F.: *Heat transfer under supercritical pressures*. In: Advances in Heat Transfer, Vol. 21, (J.P. Hartnett *et al.*, Eds.), Academic Press Inc., San Diego CA 1991, 1–53.

[5] Y.-Y. Hsu, R.W. Graham: *Transport Processes in Boiling and Two-Phase Systems. Including Near-Critical Fluids*. Hemisphere Publ. Corp., Washington DC 1976.

[6] Kurganov V.A.: *Heat Transfer and Pressure Drop in Tubes under Supercritical Pressure of the Coolant. Part 1: Specifics of the Thermophysical Properties, Hydrodynamics and Heat Transfer of the Liquid. Regimes of Normal Heat Transfer*. Thermal Engineering (English translation of Teploenergetika) **45**(1998), 3, 177–185.

[7] *REFPROP – Reference Fluid Thermodynamic and Transport Properties, Ver. 8.0*. National Institute of Standards and Technology (NIST), Boulder CO, 2007.